

## Effect of La substitution on thermal stability of $\text{ThV}_2\text{O}_7$

Mrinal. R. Pai, B.N. Wani, N.M. Gupta\*

*Applied Chemistry Division, Bhabha Atomic Research Centre, Trombay, Bombay-400085, India*

Received 1 August 2003; received in revised form 1 February 2004; accepted 10 June 2004

Available online 4 August 2004

### Abstract

The substituted samples with nominal compositions of  $\text{La}_x\text{Th}_{1-x}\text{V}_2\text{O}_{7-\delta}$  ( $x=0-0.5$ ) were synthesized for the first time by ceramic route and the phase characterization was carried out by powder XRD technique. In addition to substitution at some of the thorium sites in  $\text{ThV}_2\text{O}_7$ , the substituted samples comprised of two new phases, viz.,  $\text{Th}(\text{VO}_3)_4$  and  $\text{LaTh}(\text{VO}_4)_{3-\delta}$ . The relative amount of these three constituent phases in a particular sample depended upon the value of  $x$ . Furthermore, the DTA/TG results revealed that the presence of La led to suppression of the polymorphic behavior of  $\text{ThV}_2\text{O}_7$ . The stability of these compounds in hydrogen atmosphere was monitored using temperature programmed reduction (TPR) method. As compared to  $\text{ThV}_2\text{O}_7$  and  $\text{Th}(\text{VO}_3)_4$ , the  $\text{LaTh}(\text{VO}_4)_{3-\delta}$  phase was found to reduce at higher temperatures. © 2004 Elsevier B.V. All rights reserved.

**Keywords:** Lanthanum; Thorium vanadate; Temperature programmed reduction

### 1. Introduction

The physico-chemical and structural properties are known to play a crucial role in the catalytic properties of metal oxides. A large number of investigations [1–4] have been made on modification of these properties, so as to augment the activity, selectivity and the thermal stability of a particular oxide catalyst. With this objective in view, various mixed metal oxides, particularly of perovskite and spinel type structure, have been investigated in detail and attempts have been made to incorporate multiple cations at A or B sites of these oxide systems so as to further tailor their catalytic behavior and the stoichiometric stability during actual application. We, however, noticed that not much research has been devoted to the catalytic properties of thorium based mixed oxides, even though thoria exists as one of the largest mineral reserves, particularly in India. We have taken up research in this area by synthesizing Th–V–O mixed oxide systems with further substitutions at either A or B sites, with an intention to incorporate the inherent high catalytic activity of vanadia due to its multivalent nature and at the same time the thermal

stability of thoria. Our objective was also to demonstrate the nature of structural defects created by such substitutions and the influence of these on the catalytic behavior.

The  $\text{V}_2\text{O}_5$ – $\text{ThO}_2$  mixed oxide system is known to exhibit the formation of two stable phases viz., thorium metavanadate  $\text{Th}(\text{VO}_3)_4$  [5] and thorium pyrovanadate  $\text{ThV}_2\text{O}_7$  [6]. Out of these,  $\text{Th}(\text{VO}_3)_4$  melts at  $988^\circ\text{C}$  whereas  $\text{ThV}_2\text{O}_7$  shows a reversible polymorphic phase transition at  $878^\circ\text{C}$  prior to its melting at  $1054^\circ\text{C}$  [7]. Recently, we have reported [8–9] on the structural characteristics, thermal stability, redox properties and the catalytic activity of metavanadate of thorium,  $\text{Th}(\text{VO}_3)_4$  as a function of Mn-substitution at B sites. Formation of two new phases, viz., tetragonal  $\text{ThMn}_2(\text{VO}_4)_2\text{O}_2$  and hexagonal  $\text{ThMn}_4\text{O}_8$  was established using powder XRD and IR techniques and at the same time the catalytic activity was found to improve considerably for oxidation of carbon monoxide. In continuation of the previous study, we have attempted to synthesize the pyrochlore or  $\text{A}^{\text{IV}}\text{B}_2\text{O}_7$  type compounds of thorium and vanadium, and the influence of  $\text{La}^{3+}$  substitution at A-site over the redox behavior and catalytic activity studies of these oxides for reaction of methanol was studied and reported elsewhere [10]. In this communication our objective is to monitor the thermo-physical characteristics in these La substituted pyrochlore based ( $\text{La}_x\text{Th}_{1-x}\text{V}_2\text{O}_{7-\delta}$ )

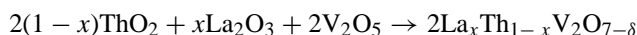
\* Corresponding author. Fax: +91 22 5505151.

E-mail address: [nmgupta@magnum.barc.ernet.in](mailto:nmgupta@magnum.barc.ernet.in) (N.M. Gupta).

samples by simultaneous Thermogravimetry (TG) and Differential thermal analysis (DTA) measurements as a function of substitution at A site. The thermal stability in hydrogen atmosphere was studied using temperature-programmed reduction (TPR) method.

## 2. Experimental

$\text{La}_x\text{Th}_{1-x}\text{V}_2\text{O}_{7-\delta}$  samples with nominal composition ( $x = 0.0\text{--}0.5$ ) were synthesized by ceramic route according to the following equation:



Preheated  $\text{La}_2\text{O}_3$  (at  $700^\circ\text{C}$ ),  $\text{ThO}_2$  (AR Grade), and  $\text{V}_2\text{O}_5$  (Aldrich make) were employed as precursors. The pellets of composite oxides were calcined in three steps; first below  $650^\circ\text{C}$  for two days to avoid the melting of  $\text{V}_2\text{O}_5$  (m.p.  $690^\circ\text{C}$ ) followed by heating at  $750^\circ\text{C}$  for three days and finally at  $900^\circ\text{C}$  for 24 h.

The samples were characterized using powder XRD (Philips Diffractometer PW 1710), equipped with a monochromator and Ni-filtered Cu  $K\alpha$  radiation. Program used for generating the lattice parameters from powder XRD pattern was POWD program version 2.2 [11]. Simultaneous TG/DTA scans of all mixed oxides were recorded on TG-DT 30 Shimadzu thermobalance with sample size of 25 mg and at a heating rate of  $10^\circ\text{C min}^{-1}$  in argon atmosphere. The reduction behavior in hydrogen atmosphere was studied by recording temperature programmed reduction (TPR) profiles with the help of a Thermoquest TPDRO-1100 analyzer. The TPR patterns were recorded in a temperature interval of  $27\text{--}900^\circ\text{C}$  (heating rate:  $6^\circ\text{C min}^{-1}$ ) and under the flow of  $\text{H}_2$  (5 vol.%) + Ar at  $20\text{ ml min}^{-1}$ .

## 3. Results and discussion

### 3.1. XRD

The XRD powder patterns for  $\text{La}_x\text{Th}_{1-x}\text{V}_2\text{O}_{7-\delta}$ ,  $0 \leq x \leq 0.5$  compositions are shown in Fig. 1. Most of the lines in the XRD pattern of  $\text{ThV}_2\text{O}_7$  (curve a) matched with the reported pattern of orthorhombic  $\text{ThV}_2\text{O}_7$  with  $a_0 = 7.261\text{ \AA}$ ,  $b_0 = 6.964\text{ \AA}$  and  $C_0 = 22.80\text{ \AA}$  with  $z = 8$ , (JCPDS 24-1330). Few additional lines at  $23.5^\circ$ ,  $15.8^\circ$ ,  $24.0^\circ$ , and  $33.5^\circ$  of low intensity are also noticed in Fig. 1a, which do not match with the XRD pattern of  $\text{ThV}_2\text{O}_7$ . These XRD lines may be identified with the tetragonal  $\text{Th}(\text{VO}_3)_4$  phase (JCPDS 31-1389). Thus, the formation of  $\text{Th}(\text{VO}_3)_4$  phase was found to be inevitable while synthesizing  $\text{ThV}_2\text{O}_7$  by ceramic route. In addition to the XRD lines mentioned above, the patterns of the La substituted composition (Fig. 1b–e) reveal the presence of few additional lines at  $2\theta = 15.84^\circ$ ,  $24.12^\circ$ ,  $32.31^\circ$  and  $47.88^\circ$  (marked \*). These lines are not associated with either of  $\text{La}_2\text{O}_3$  and  $\text{La}(\text{OH})_3$ . We may also mention that the most

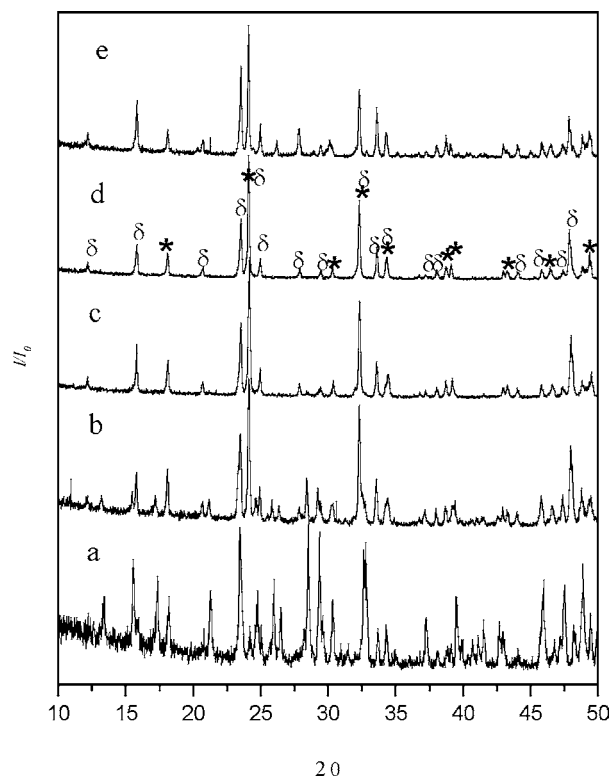


Fig. 1. XRD powder patterns of  $\text{La}_x\text{Th}_{1-x}\text{V}_2\text{O}_{7-\delta}$  as a function of  $x$  ( $0.0 < x < 0.5$ ). \*Peaks due to  $\text{LaTh}(\text{VO}_4)_{3-\delta}$  and  $\delta\text{Th}(\text{VO}_3)_4$  phase.

intense XRD line of  $\text{ThV}_2\text{O}_7$  appears at  $2\theta$  value of  $28.5^\circ$ . On the other hand, the most intense peak in XRD pattern of  $\text{La}_{0.2}\text{Th}_{0.8}\text{V}_2\text{O}_{7-\delta}$  is noticed at  $24.1^\circ$  and not at  $28.5^\circ$ , indicating the appearance of a new phase. On scrutiny, this new phase was found to be iso-structural with  $\text{PbLaTh}(\text{VO}_4)_3$  [12] and can be attributed to the formation of a new  $\text{LaTh}(\text{VO}_4)_{3-\delta}$  phase. Fig. 2 exhibits the selected region of XRD pattern so as to highlight the presence of  $\text{ThV}_2\text{O}_7$  phase. We thus observe that the XRD lines of the original pyrovanadate phase are still present on substitution of up to 30% of  $\text{Th}^{4+}$  by  $\text{La}^{3+}$ , though with progressive decrease in intensity (Fig. 2). However, the lines due to  $\text{ThV}_2\text{O}_7$  phase are found to disappear in  $\text{La}_x\text{Th}_{1-x}\text{V}_2\text{O}_{7-\delta}$  ( $0.3 < x < 0.5$ ) compositions and these samples are thus comprised of only two phases viz.,  $\text{Th}(\text{VO}_3)_4$  (marked as  $\delta$ ) and the above-mentioned new phase (marked as \*), as shown in curve d of Fig. 1. The XRD reflections of this hitherto unreported phase  $\text{LaTh}(\text{VO}_4)_{3-\delta}$  were separated and indexed using indexing program, and these data are included in Table 1. In conclusion, the synthesized La–Th–V oxides may thus be regarded as a mixture of  $\text{ThV}_2\text{O}_7$ ,  $\text{LaTh}(\text{VO}_4)_{3-\delta}$  and  $\text{Th}(\text{VO}_3)_4$  phases, the relative contents of which depend upon the value of  $x$ .

### 3.2. TG/DTA studies

Simultaneous TG/DTA curves of  $\text{ThV}_2\text{O}_7$  and  $\text{Th}(\text{VO}_3)_4$ , recorded in argon atmosphere, are presented in Fig. 3. TG scans of both the sample do not show any weight loss indi-

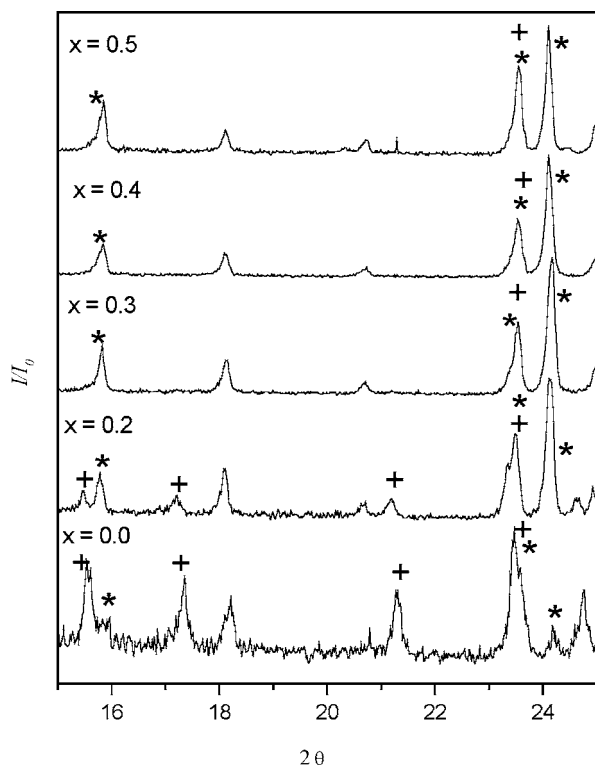


Fig. 2. Selected XRD lines of  $\text{La}_x\text{Th}_{1-x}\text{V}_2\text{O}_{7-\delta}$  as a function of  $x$  ( $0.0 < x < 0.5$ ) indicating the presence of  $\text{ThV}_2\text{O}_7$  phase. \*Peaks due to  $\text{Th}(\text{VO}_3)_4$  and + $\text{ThV}_2\text{O}_7$  phase.

cating that once these samples are formed, they do not pick up either of moisture or  $\text{CO}_2$  and are stable mixed oxides. But the corresponding DTA curves showed some multiple endotherms indicating thereby that they are not simply due to decomposition but arise either because of certain phase transformation or due to melting of thorium vanadates. On heating, DTA curve of  $\text{Th}(\text{VO}_3)_4$  (Fig. 3a) exhibits a sharp endotherm at  $982^\circ\text{C}$  which may be attributed to the peritectic melting of  $\text{Th}(\text{VO}_3)_4$  and a broad endotherm in temperature

Table 1

Powder XRD pattern of  $\text{LaTh}(\text{VO}_4)_{3-\delta}$ , system tetragonal:  $a = 7.3803 \text{ \AA}$ ,  $c = 6.5375 \text{ \AA}$ ,  $V = 356.09 \text{ \AA}^3$

Line number	$d$ -Spacing ( $\text{Å}$ )		$I/I_0$	$h$	$k$	$l$
	Observed	Calculated				
1	4.8990	4.8937	20	1	0	1
2	3.6910	3.6902	100	2	0	0
3	2.9480	2.9464	8	2	1	1
4	2.7700	2.7702	67	1	1	2
5	2.6120	2.6093	19	2	2	0
6	2.3242	2.3225	12	2	1	2
7	2.0904	2.0900	9	1	0	3
8	1.9536	1.9534	9	3	2	1
9	1.8450	1.8451	23	4	0	0
10	1.8187	1.8185	5	2	1	3
11	1.7252	1.7264	4	4	1	1
12	1.6501	1.6503	11	4	2	0
13	1.6338	1.6344	4	0	0	4
14	1.5356	1.5356	12	3	3	2

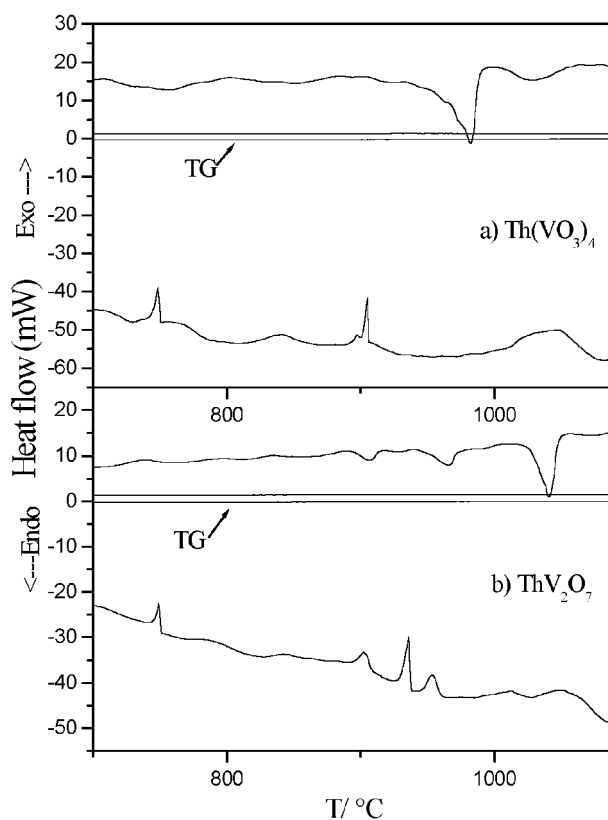


Fig. 3. Simultaneous TG/DTA curves of  $\text{ThV}_2\text{O}_7$  and  $\text{Th}(\text{VO}_3)_4$ .

region  $1000\text{--}1060^\circ\text{C}$  which could be due to crossing of the liquidus boundary as indicated by the phase diagram. The corresponding cooling scan showed four exotherms: a broad one above  $1000^\circ\text{C}$ , and relatively sharper ones at  $905$ ,  $840$  and  $749^\circ\text{C}$ . DTA curve of  $\text{ThV}_2\text{O}_7$  (Fig. 3b) showed three endotherms at  $906$ ,  $966$  and  $1040^\circ\text{C}$ . The first and the third endotherms are attributed to phase transition and melting of  $\text{ThV}_2\text{O}_7$ , respectively, whereas the one at  $966^\circ\text{C}$  is due to melting of  $\text{Th}(\text{VO}_3)_4$  phase present as an impurity. On cooling one ends up with multiple exotherms at  $950$ ,  $930$ ,  $900$  and  $740^\circ\text{C}$ . When we refer to phase diagram of  $\text{V}_2\text{O}_5\text{--ThO}_2$  [2] it shows peritectic melting of  $\text{ThV}_2\text{O}_7$  and  $\text{Th}(\text{VO}_3)_4$ . Therefore, when these compounds are heated above their melting point, the formation of thorium vanadium oxides with various compositions during cooling, is observed. This is clearly reflected in the broad nature of DTA endotherms recorded during the heating and also the exotherms recorded during the cooling cycles for all Th–V oxides. The corresponding TG curves do not show any weight loss indicating the absence of free  $\text{V}_2\text{O}_5$ . Since free  $\text{V}_2\text{O}_5$  melts at  $690^\circ\text{C}$  and vaporizes on further heating, that reflects as weight loss in the TG curve. Additional sharp exothermic peak at  $750^\circ\text{C}$  is also noticeable in the cooling cycle, which is found to be reproducible in subsequent heating and cooling cycles and could be due to eutectic melting. To ensure the nature of above exothermic peak, a fresh sample was heated up to  $800^\circ\text{C}$  i.e. below phase transition temperature and cooled back to room tem-

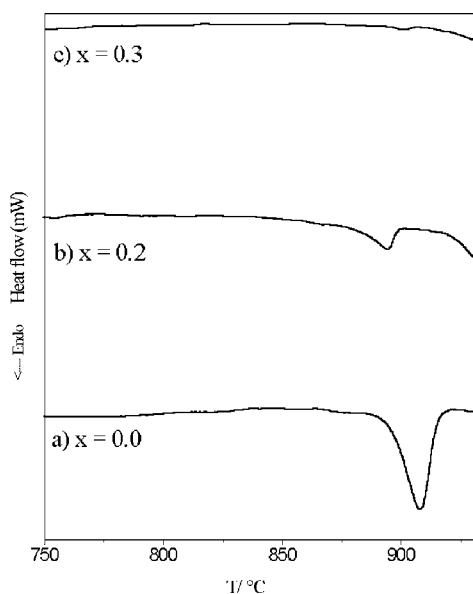


Fig. 4. DTA curves of  $\text{La}_x\text{Th}_{1-x}\text{V}_2\text{O}_{7-\delta}$  compositions to show phase transition.

perature. It was observed that the above mentioned heat effect was missing; indicating that the exothermic effect at  $750^\circ\text{C}$  arises only after melting.

The DTA scan of  $\text{La}_{0.2}\text{Th}_{0.8}\text{V}_2\text{O}_{7-\delta}$  shows a drastic decrease in the intensity of the phase transition peak but this trend vanishes completely for the sample with  $x = 0.3$  (Fig. 4). This phase transformation could be suppressed either because of the substitution of La into the lattice of  $\text{ThV}_2\text{O}_7$  phase or due to disappearance of  $\text{ThV}_2\text{O}_7$  phase. XRD results showed the presence of  $\text{ThV}_2\text{O}_7$  phase and therefore a systematic shift in  $T_{\text{max}}$  from  $906$  to  $893^\circ\text{C}$  in Fig. 4 may be taken as an evidence of La substitution into  $\text{ThV}_2\text{O}_7$  lattice. DTA curves during heating and cooling of  $\text{La}_x\text{Th}_{1-x}\text{V}_2\text{O}_{7-\delta}$  were also recorded (Fig. 5).  $\text{La}_{0.4}\text{Th}_{0.6}\text{V}_2\text{O}_{7-\delta}$  and  $\text{La}_{0.5}\text{Th}_{0.5}\text{V}_2\text{O}_{7-\delta}$  compositions contain only two phases viz.,  $\text{Th}(\text{VO}_3)_4$  and  $\text{LaTh}(\text{VO}_4)_{3-\delta}$  and the DTA curves show that the melting peak of  $\text{Th}(\text{VO}_3)_4$  was shifted to lower temperature by  $20^\circ\text{C}$  (Table 2). Since the melting peak of  $\text{Th}(\text{VO}_3)_4$  shifts to lower temperature in  $x = 0.4$  and  $0.5$  samples, it is likely that a part of La also occupies the lattice positions in  $\text{Th}(\text{VO}_3)_4$  phase. It is also observed that there is no corresponding exothermic peak for the melting around  $900^\circ\text{C}$  and the only exotherm is

Table 2

DTA peak temperatures of  $\text{La}_x\text{Th}_{1-x}\text{V}_2\text{O}_{7-\delta}$  in argon atmosphere

Compositions	Endothermic peak temperature during heating ( $^\circ\text{C}$ )	Exothermic peak temperature during cooling ( $^\circ\text{C}$ )
$\text{ThV}_2\text{O}_7$	906, 966, 1040	950, 922, 692
$\text{La}_{0.2}\text{Th}_{0.8}\text{V}_2\text{O}_{7-\delta}$	892, 953, 1050	1060, 982, 907, 682
$\text{La}_{0.3}\text{Th}_{0.7}\text{V}_2\text{O}_{7-\delta}$	960	893, 721
$\text{La}_{0.4}\text{Th}_{0.6}\text{V}_2\text{O}_{7-\delta}$	904, 941	813, 670
$\text{La}_{0.5}\text{Th}_{0.5}\text{V}_2\text{O}_{7-\delta}$	912, 944	697
$\text{Th}(\text{VO}_3)_4$	982	905, 745

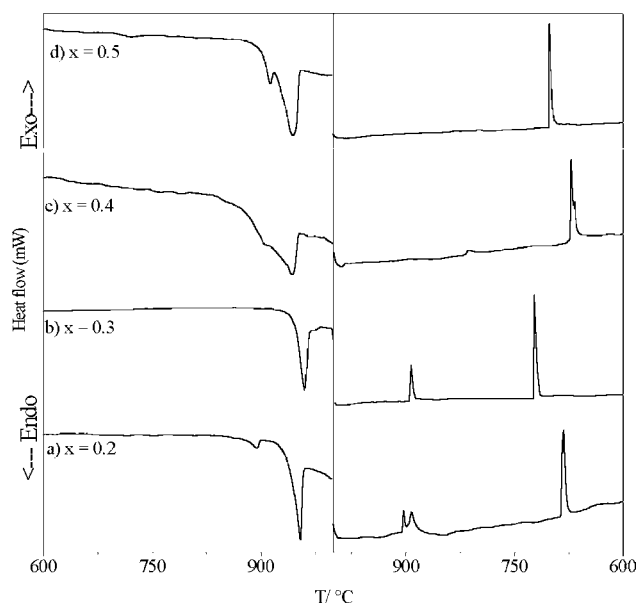


Fig. 5. DTA curves of  $\text{La}_x\text{Th}_{1-x}\text{V}_2\text{O}_{7-\delta}$  compositions with the varying values of  $x$ .

observed between  $660$  and  $700^\circ\text{C}$ . This could be attributed to peritectic melting, which on cooling may give rise to some ternary eutectic formation in La–Th–V oxides. Further, as compared to pure thorium pyrovanadate, the La doped samples showed melting at a lower temperature (Table 2) suggesting that as the concentration of La increases, it enters first into  $\text{ThV}_2\text{O}_7$  up to  $x = 0.3$  and stabilizes in its low temperature form. For higher values of  $x$ , La also starts substituting into  $\text{Th}(\text{VO}_3)_4$  phase as indicated by the shifts observed in melting points.

### 3.3. TPR studies

Since the thorium based oxides are known to exhibit high catalytic activity for various organic reactions, the effect of substitution on the reduction behavior of our samples was monitored by recording TPR profiles. TPR profiles of  $\text{La}_x\text{Th}_{1-x}\text{V}_2\text{O}_{7-\delta}$  samples are compiled in Fig. 6. As shown in Fig. 6a, the TPR profile of  $\text{ThV}_2\text{O}_7$  comprises of one broad band with the temperature maximum ( $T_{\text{max}}$ ) at around  $750^\circ\text{C}$  and a shoulder at  $650^\circ\text{C}$ . As La-doping increases up to  $x = 0.3$ , this reduction band shifts to lower temperature and at the same instant the intensity of shoulder band increases at the cost of the main peak. The development of an additional band at  $900^\circ\text{C}$  is also noticeable in TPR spectra of substituted samples (Fig. 6b–e). The TPR profile of sample with  $x = 0.4$ , which contains only  $\text{Th}(\text{VO}_3)_4$  and  $\text{LaTh}(\text{VO}_4)_{3-\delta}$  phase, exhibits two broad bands, first in the temperature interval of  $590$ – $804^\circ\text{C}$  and second one in  $829$ – $960^\circ\text{C}$ . We have earlier reported that the TPR profiles of  $\text{Th}(\text{VO}_3)_4$  contain two overlapping bands of almost equal intensity and with temperature maximum ( $T_m$ ) at  $640$  and  $740^\circ\text{C}$ . Hence the first broad band of  $\text{La}_x\text{Th}_{1-x}\text{V}_2\text{O}_{7-\delta}$  com-

Table 3  
Hydrogen consumption by  $\text{La}_x\text{Th}_{1-x}\text{V}_2\text{O}_{7-\delta}$  during TPR run

Composition	First peak		Second peak		Total $\text{H}_2$ consumption ( $\mu\text{mol/gm}$ )
	Temperature interval ( $^\circ\text{C}$ )	$\text{H}_2$ consumption ( $\mu\text{mol/gm}$ )	Temperature interval ( $^\circ\text{C}$ )	$\text{H}_2$ consumption ( $\mu\text{mol/gm}$ )	
$\text{ThV}_2\text{O}_7$	580–860	2875	–	–	2875
$\text{La}_{0.2}\text{Th}_{0.8}\text{V}_2\text{O}_{7-\delta}$	580–814	3100	844–940	504	3605
$\text{La}_{0.3}\text{Th}_{0.7}\text{V}_2\text{O}_{7-\delta}$	580–775	3116	834–940	690	3807
$\text{La}_{0.4}\text{Th}_{0.6}\text{V}_2\text{O}_{7-\delta}$	591–804	2853	829–960	854	3708
$\text{La}_{0.5}\text{Th}_{0.5}\text{V}_2\text{O}_{7-\delta}$	600–770	2889	780–940	524, 672	4085
$\text{Th}(\text{VO}_3)_4$	540–750	5563	–	–	5563

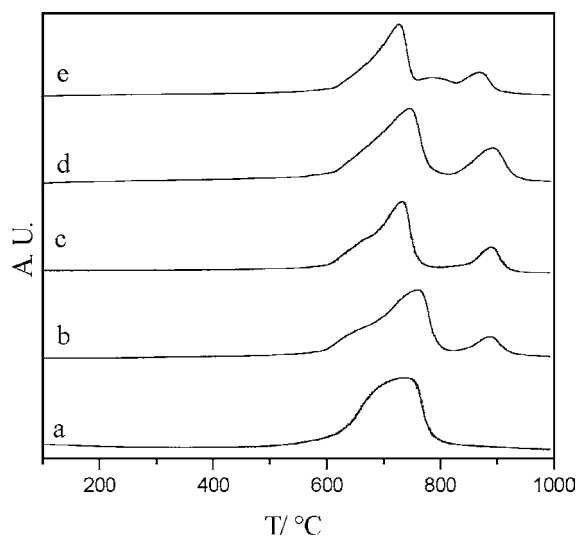


Fig. 6. TPR plots of  $\text{La}_x\text{Th}_{1-x}\text{V}_2\text{O}_{7-\delta}$  samples as a function of  $x$ .

positions was assigned to reduction of  $\text{Th}(\text{VO}_3)_4$  and the later one due to reduction of  $\text{LaTh}(\text{VO}_4)_{3-\delta}$ . The total amount of hydrogen consumption during these first and second peaks is given in Table 3. During reduction, the amount of hydrogen consumed by  $\text{ThV}_2\text{O}_7$  was almost half as compared to  $\text{Th}(\text{VO}_3)_4$ . These results find a correlation with the presence of two times higher V:Th ratio in  $\text{Th}(\text{VO}_3)_4$  as compared to  $\text{ThV}_2\text{O}_7$ , vanadium being the only reducible species in both these compositions. This explains why the amount of hydrogen consumed for reducing the former is half as compared to later sample (Table 3). As seen in the data of Table 3, the total hydrogen consumption in case of the substituted  $\text{La}_x\text{Th}_{1-x}\text{V}_2\text{O}_{7-\delta}$  compositions remained almost the same as the vanadium content in these samples is constant. Thus, the TPR results in Fig. 6 in conjunction with XRD data clearly indicate that when a sample of mixed composition is heated in hydrogen atmosphere,  $\text{Th}(\text{VO}_3)_4$  undergoes reduction in first stage followed by that of  $\text{ThV}_2\text{O}_7$  and  $\text{LaTh}(\text{VO}_4)_{3-\delta}$  reduces in last stage. We can thus infer that as compared to  $\text{VO}_3^-$  and  $\text{V}_2\text{O}_7^{4-}$  anions,  $\text{VO}_4^{3-}$  anion reduces at a higher temperature.

#### 4. Conclusions

La substitution in  $\text{ThV}_2\text{O}_7$  invariably resulted into mixed phase compositions. La doping resulted in: (a) development of a new tetragonal orthovanadate phase,  $\text{LaTh}(\text{VO}_4)_{3-\delta}$  which reduces above  $900^\circ\text{C}$ ; (b) lowering in phase transition for samples with  $x = 0-0.2$  indicating that part of La has entered in  $\text{ThV}_2\text{O}_7$  lattice and (c) shift of the overall TPR profile to lower temperature indicating the ease of reduction process due to oxygen ion vacancies generated in  $\text{V}_2\text{O}_7^{4-}$  chains. Finally, in case of Th–V–O system when all the three phases are present together, the reduction process occurs in this order: first metavanadate, then pyrovanadate and finally orthovanadate.

#### Acknowledgement

We thank Dr. R.K. Mishra of Applied Chemistry Division and Dr. J. Radhakrishnan of Fuel Chemistry Division, BARC for recording DTA curves and Dr. S.R. Bhardwaj of Applied Chemistry Division for useful discussion.

#### References

- [1] G. Busca, L. Lietti, G. Ramis, F. Berti, *Appl. Catal. B: Environ.* 18 (1998) 1.
- [2] L.G. Tejuca, J.L.G. Fierro (Eds.), *Properties and Applications of Perovskite type Oxides*, Marcel Dekker, New York, 1993.
- [3] C.S. Swamy, J. Christopher, *Catal. Rev. Sci. Eng.* 34 (1992) 40.
- [4] V.C. Belessi, C.N. Costa, T.V. Bakas, T. Anastasiadou, P.J. Pomonis, A.M. Efstathiou, *Catal. Today* 59 (2000) 347.
- [5] A. Tabuteau, A. Cousson, M. Pages, *Acta Cryst. B* 35 (1979) 2000.
- [6] G. Le Flem, P. Hagenmuller, *Rev. Hautes Temp. Refrac.* 1 (1964) 149.
- [7] S. Launay, P. Mahe, M. Quarton, F. Robert, *J. Solid State Chem.* 97 (1992) 305.
- [8] M.R. Pai, B.N. Wani, N.M. Gupta, *J. Mater. Sci. Lett.* 21 (2002) 118.
- [9] M.R. Pai, B.N. Wani, N.M. Gupta, *Prog. Cryst. Growth Charac.* 45 (2002) 107.
- [10] M.R. Pai, B.N. Wani, A.D. Belapurkar, N.M. Gupta, *J. Mol. Catal. A.*, accepted for publication.
- [11] V.S. Jakkal, BARC, Mumbai, India, private communication.
- [12] M.A. Nabar, B.G. Mhatre, *J. Solid State Chem.* 45 (1982) 135.